First Principles Calculation of the Interdiffusion Coefficient in Binary Alloys

A. Van der Ven and G. Ceder

Department of Materials Science and Engineering, Massachusetts Institute of Technology, 77 Massachusetts Ave., Cambridge, Massachusetts 02139, USA

(Received 28 January 2004; revised manuscript received 14 December 2004; published 3 February 2005)

The atomic mechanisms of diffusion in alloys are complex due to the variations of migration energies with environment and the correlations induced by short-range order between the different components. We present a first-principles approach for calculating vacancy-mediated diffusion coefficients in crystalline binary alloys and apply it to obtain the interdiffusion coefficient of $\mathrm{Al}_{(1-x)}\mathrm{Li}_x$. The rigorous treatment of atomic migration indicates that short- and long-range order induces strongly correlated migration mechanisms that deviate from random walk behavior.

DOI: 10.1103/PhysRevLett.94.045901 PACS numbers: 66.30.Dn, 61.66.Dk, 66.30.Ny

Technologically important materials often derive their properties from kinetically formed microstructures. Atomic diffusion plays a key role in determining the rate and mechanism of nonequilibrium phenomena in alloys. Many phase transformations in alloys involve the redistribution of different species between the growing and consumed phases.

While first-principles thermodynamics has been very successful in predicting the equilibrium structure and properties of materials [1], considerably less has been done on first-principles kinetics in alloys. In this Letter, we present an approach to predict, from first principles, interdiffusion behavior in alloys and apply it to the Al-Li system. Although self-diffusion or dilute impurity diffusion in elemental solids is governed by a single migration barrier and attempt frequency, the vacancy-mediated interdiffusion in alloys is considerably more complex [2]. The frequencies with which different atomic species can exchange with an adjacent vacancy are not all the same. Furthermore, multicomponent solids are characterized by different states of long- and short-range order as a function of composition and temperature with the vacancies energetically preferring certain types of order above others. Spatial variations in atomic order constrict the motion of vacancies, thereby affecting atomic mobility. Experimental determinations of the macroscopic activation barrier represent a complex average of these microscopic quantities.

Here we present a method to calculate interdiffusion coefficients from first principles in binary alloys in which diffusion is mediated by vacancies. The method includes a full parameterization of the dependence of the energy and activation barrier on the configuration of the different components of the solid, as well as a formally correct analysis of interdiffusion. Our results on Al-Li indicate that the interdiffusion coefficient is strongly affected by hopping correlations induced by the short- and long-range order in the system, making simple diffusion models based on single migration barriers unreliable.

We focus on the fcc based Al-Li alloy. $\mathrm{Al}_{(1-x)}\mathrm{Li}_x$ exhibits a metastable ordered $L1_2$ phase at $x = 0.25$, which when precipitated out in an Al rich matrix enhances the mechanical properties of fcc based Al-Li alloys [3].

In a binary crystalline solid containing vacancies, such as the Al-Li alloy, the fluxes J_i of the different components ($i =$ Al or Li) are related to gradients in concentration, ∇C_j, of component j (C is the number of particles per unit volume) according to $J_i = \sum_j - D_{ij} \nabla C_j$. The matrix of diffusion coefficients D_{ij} can be expressed as a product of a kinetic factor $\mathbf{L}$ and a thermodynamic factor $\mathbf{\Theta}$ as $\mathbf{D} = \mathbf{L}\mathbf{\Theta}$. The components of $\mathbf{L}$ and $\mathbf{\Theta}$ for a d-dimensional solid with volume V can be derived with a Kubo-Green formalism [4] as $\Theta_{ij} = \partial \tilde{\mu}_i / \partial C_j$ and

$$L_{ij} = \frac{\langle (\sum_{\zeta} \Delta \vec{R}^i_{\zeta}(t))(\sum_{\xi} \Delta \vec{R}^j_{\xi}(t)) \rangle}{(2d) t V k_B T}, \tag{1}$$

with $\Delta \vec{R}^i_{\zeta}$ the vector connecting the endpoints of the trajectory of atom ζ of type i after a time t. The quantity $\tilde{\mu}_i$ is the difference in the chemical potential of component i and the vacancy chemical potential [5]. The brackets in the expression for L_{ij} refer to an ensemble average.

In the dilute vacancy limit, diagonalization of the $\mathbf{D}$ matrix leads to a decoupling of diffusion into two modes; one for density relaxation due to a nonuniform vacancy concentration and the other to *interdiffusion*[6]. The eigenvalue of interdiffusion is a measure of the rate with which the two components of the alloy intermix when concentration gradients are present. It is therefore also the appropriate coefficient that enters Fick's equation for interdiffusion in a binary diffusion couple.

An accurate kinetic model needs to include both the correct thermodynamics of the system—so that it evolves to the correct equilibrium state—as well as the proper atomic mobilities and diffusion events. The configurational thermodynamics can be modeled rigorously with a cluster expansion and Monte Carlo simulations through a procedure that is well established [1]. The cluster expansion, essentially a lattice model formalism, is used to describe the configurational dependence of the energy in the Al-Li-

0031-9007/05/94(4)/045901(4)$23.00

vacancy system by assigning occupation variables [7] σ_m to each lattice point m $(+1(-1)$ if Li (Al) is at site m and 0 if m is vacant), and expanding the configurational energy in polynomials of these occupation variables. Our cluster expansion for the configurational energy of the fcc Al-Li alloy was made *ab initio* by fitting the coefficients of the polynomial basis functions to first-principles local density approximation (LDA) energies of more than 70 fully relaxed Al-Li arrangements on fcc [8]. The presence of a dilute concentration of vacancies in a binary alloy can be treated by augmenting the conventional binary cluster expansion with a local cluster expansion [9]. For fcc Al-Li, the coefficients of the vacancy local cluster expansion were fit to the LDA energies of 23 Al-Li configurations surrounding a vacancy as calculated within a 107 atoms supercell [9]. The LDA (Perdew-Zunger parametrization) calculations were performed with the Vienna *ab initio* simulation package (VASP) pseudopotential code [8] using ultrasoft pseudopotentials.

Applying Monte Carlo simulations to the first-principles cluster expansion of fcc Al-Li predicts the experimentally observed $L1_2$ ordered phase at $x = 0.25$ [10] [Fig. 1(a)]. The equilibrium vacancy concentration [Fig. 1(b)] was calculated with grand canonical Monte Carlo simulations, setting the vacancy chemical potential to zero. While more or less constant in the solid solution phase, the calculated equilibrium vacancy concentration at 600 K varies rapidly with alloy concentration in the ordered phase. Figure 1(c) shows that the equilibrium lithium concentration within the first nearest neighbor shell of a vacancy is lower than the average bulk concentration [dashed straight line in Fig. 1(c)], while the lithium concentration in the second nearest neighbor shell of a vacancy is slightly enhanced over the average lithium concentration. Hence, vacancies prefer to be surrounded by Al. In fact, our first-principles LDA calculations on 107 atom supercells show that a vacancy energetically repels a lithium atom in otherwise pure Al, with a decrease in energy by 80 meV as a single Li is taken from a vacancy's first nearest neighbor shell to its fourth nearest neighbor shell [11]. In the $L1_2$ phase, the Monte Carlo simulations predict that the vacancy predominantly occupies the lithium sublattice on which the vacancy is able to surround itself in its first nearest neighbor shell exclusively with Al.

The kinetic component of diffusion in crystalline alloys can be characterized as a Markov process, whereby migrating atoms hop between well defined crystallographic sites and thermalize before hopping again [4]. The rate Γ with which individual hops occur is to a good approximation given by transition state theory [12] according to $\Gamma = \nu^* \exp(-\Delta E_b/k_B T)$, where ν^* is a vibrational prefactor and ΔE_b is the activation barrier. The activation barrier ΔE_b is the difference in the energy of the activated state, E_{act}, and that of the initial state of the hop, E_{initial}. In an alloy, ΔE_b depends on the local atomic arrangement, as both the energy of the initial state and activated state are configuration dependent. ΔE_b also depends on the direction of the hop, making it difficult to treat its configuration dependence with a cluster expansion. This formal difficulty can be overcome, however, by introducing a *kinetically resolved activation barrier* (KRA) [13] defined as $\Delta E_k = E_{\text{act}} - 1/2(E_{\text{initial}} + E_{\text{final}})$ with E_{final} the energy of the final state of the hop. ΔE_k is direction independent making an unambiguous expansion with a local cluster expansion possible [13]. The activation barrier can then be reconstructed according to $\Delta E_b = \Delta E_k - 1/2(E_{\text{initial}} - E_{\text{final}})$ in which each separate term is parameterized by a cluster expansion: ΔE_k by a local cluster expansion, and E_{initial} and E_{final} by the alloy cluster expansion for the configurational energy.

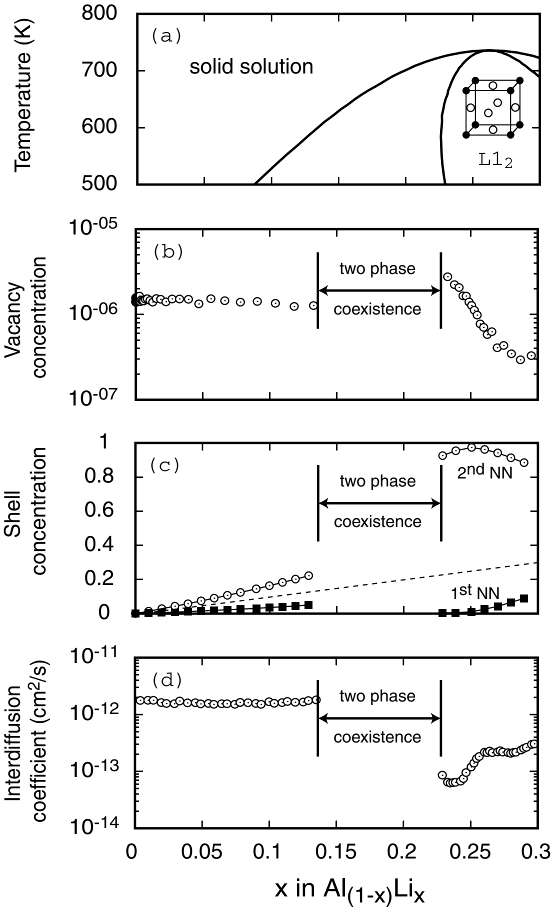

FIG. 1. (a) Calculated phase diagram of fcc $\mathrm{Al}_{(1-x)}\mathrm{Li}_x$ alloy showing stability of the metastable $L1_2$ ordering at $x = 0.25$. (b) Variation of the equilibrium vacancy concentration with x ($T = 600$ K). (c) Equilibrium Li concentration in the first (filled squares) and second (empty circles) nearest neighbor (NN) shells around a vacancy as a function of x. (d) Calculated interdiffusion coefficient at 600 K.

We calculated several KRA barriers for Al and Li hops into an adjacent vacancy with LDA using 107 atom supercells for ten representative Al-Li arrangements at different concentrations (six different arrangements around a migrating Al and four around a migrating Li; several arrangements were with dilute Li concentrations and the remaining were in the $L1_2$ ordered phase at $x = 0.25$). While the calculated ΔE_k for Li or Al do not vary strongly over the ten configurations considered (a variation of at most 60 meV which is of the order of the numerical accuracy of the first-principles calculations), they differ by almost 200 meV depending on whether Al or Li performs the hop. For Al, first-principles calculated values for ΔE_k^{Al} for different configurations and concentrations were all in the vicinity of 600 meV, while for Li, calculated values for ΔE_k^{Li} ranged around 400 meV.

To estimate ν^*, we used the local harmonic approximation [14] and considered only the Einstein vibrational frequencies of the migrating atom in the initial and activated state. The local frequencies were calculated for both an Al and a Li next to a vacancy in a 107 atom supercell of pure Al. Force constants for the migrating atoms were calculated by perturbing them by 0.05 Å from their position at the initial state and the saddle point (activated state). We found that $\nu_{\mathrm{Al}}^* \approx 4.5 \times 10^{13}$ Hz and $\nu_{\mathrm{Li}}^* \approx 7.0 \times 10^{13}$ Hz.

The first-principles results so far indicate a trade-off between thermodynamics and kinetics. Thermodynamically, the vacancy repels Li, preferring Al in its nearest neighbor shell [Fig. 1(c)]. In contrast, the activation barrier for Li exchanges with a neighboring vacancy is lower than that for Al. As a result, though Li atoms exchange more frequently with an adjacent vacancy than Al, thermodynamically, Li atoms have less access to vacancies. We can evaluate the effect of these competing tendencies quantitatively by calculating the interdiffusion coefficient using kinetic Monte Carlo simulations [15] to calculate L_{ij} and grand canonical Monte Carlo simulations to calculate Θ_{ij}. Within the kinetic Monte Carlo simulations, activation barriers ΔE_b were calculated by setting $\Delta E_k^{\mathrm{Al}} = 600$ meV and $\Delta E_k^{\mathrm{Li}} = 410$ meV for all concentrations and local environments and using the cluster expansions to calculate the environment dependence of E_{initial} and E_{final}.

Figure 1(d) illustrates the concentration dependence of the calculated interdiffusion coefficient at 600 K. Between $x = 0$ and $x = 0.15$ [solid solution, see Fig. 1(a)] the calculated interdiffusion coefficient varies negligibly with concentration while it drops by more than an order of magnitude in the ordered $L1_2$ phase (x greater than 0.23) due to the strong thermodynamic tendency of the vacancy to reside on the Li sublattice of $L1_2$, which severely restricts its mobility. Experimental estimates of the diffusion coefficient of the solid solution at 200° C yield a value of 6.8×10^{-15} cm^2/s [16], which compares to a calculated value at the same temperature of 2×10^{-15} cm^2/s. Because of the exponential dependence on ΔE_b, errors as small as 50 meV on activation barriers lead to a 3.5 factor error on the diffusion coefficient at 200° C.

Correlation factors f, which measure the efficiency of tracer diffusion relative to that of a random walker performing the same number of hops, offer valuable information about microscopic diffusion mechanisms [2]. Figure 2 illustrates strong variations in f with composition for both the vacancy and Li. The effectiveness of vacancy diffusion significantly decreases as Li is added to the system. In the ordered $L1_2$ phase, even stronger correlated diffusion is evident for each of the species, with significant reductions in mobility as compared to a random walker.

Insight about the variations in f can be obtained by tracking the frequencies of the different angles between successive hops of the vacancy. In fcc, there are five possible angles between successive hops: 0° (return hop), 180° (forward hop), 60°, 120°, and 90°. For perfectly random diffusion the frequencies with which each hop occur in fcc are $1/12$ for the 0° and 180° angles, $1/3$ for the 60° and 120° angles, and $1/6$ for the 90° angles. Figure 3 shows that as the Li concentration increases, the frequency of the 0° angle between successive hops of the vacancy increases dramatically. This arises from the large difference between Li and Al exchange frequencies with a vacancy. Once a wandering vacancy encounters an isolated fast diffuser (Li in this case) it will on average perform many back and forth exchanges before moving on. In fact, as the Li concentration increases, the fraction of vacancy exchanges with Li rapidly dominate at the expense of vacancy exchanges with Al. The frequent back and forth exchanges between the vacancy and dilute fast diffusers significantly constricts the extent of the vacancy's trajectory, leading to a small correlation factor for both the vacancy and Li (see Fig. 2).

Thermodynamic short-range order also plays an important role in affecting correlations between hops. For dilute Li concentrations, a vacancy performing many back and forth exchanges with an isolated Li can break away from that Li by exchanging with a neighboring, slower diffusing Al atom. However, to preserve energetically favored short-range order, there are differences in the frequencies between the 60° and 120° angles for successive hops of a vacancy (Fig. 3). For a vacancy which first exchanges with

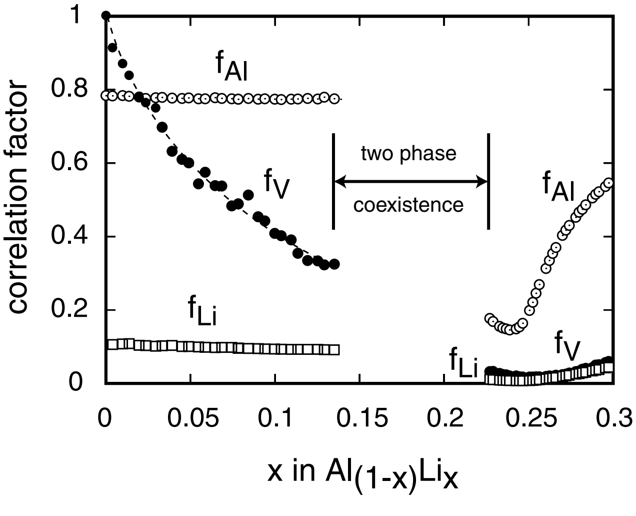

FIG. 2. Correlation factors for $\mathrm{Al}_{(1-x)}\mathrm{Li}_x$ alloy at 600 K.

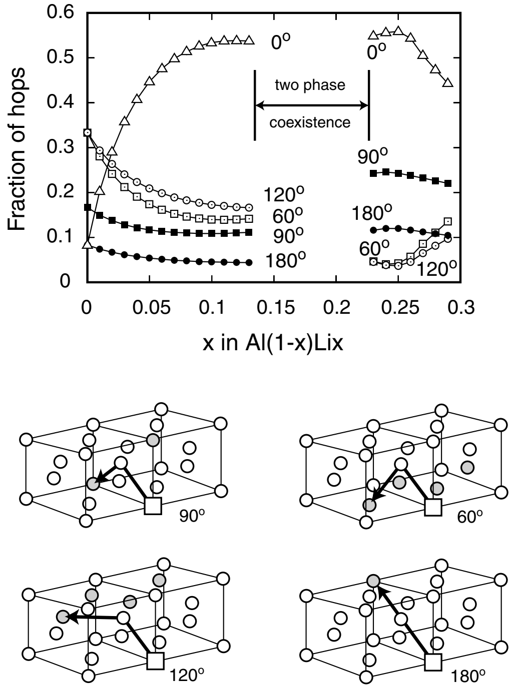

FIG. 3. Frequencies of the different possible angles between successive hops of a vacancy as a function of x.

a Li and then with an Al, the 60° angle between successive hops keeps the vacancy next to the Li which is thermodynamically unfavored, while a 120° angle between the two hops relegates the Li to the third nearest neighbor shell of the vacancy, which is thermodynamically preferred. Hence the 120° angle between successive hops occurs more frequently than the 60° angle at dilute Li concentrations.

In $L1_2$ Al_3Li, where the vacancy energetically prefers the Li sublattice, thermodynamics plays an even more significant role. While back and forth hops by the vacancy still dominate, the frequencies of the 180° and 90° angles between successive hops of the vacancy increase significantly over their random walk values. This arises from the fact that the lithium sublattice of $L1_2$ occupies the corner points of the cubic fcc unit cell and the 180° and 90° angles between successive hops return a vacancy initially on the Li sublattice (where it predominantly resides) back to another site of the Li sublattice of $L1_2$. This is not the case for the 60° and 120° angles, which therefore have very low frequencies of occurrence in $L1_2$.

While the correlation factor of Al is also small in $L1_2$, it increases rapidly beyond $x = 0.25$. Below $x = 0.25$, the vacancy primarily hops back and forth between the same lithium sublattice site and nearest neighbor aluminum sublattice sites, since the departure from the Li sublattice tends to create Al antisite defects. Above $x = 0.25$, excess lithium must occupy sites on the Al sublattice. Vacancies, which leave the Li sublattice are then more likely to do so by exchanging with one of the excess Li on the Al sublattice. The driving force for the vacancy to hop back to its original site is no longer as large as when it exchanges with an Al, causing the vacancy to more freely wander over the Li sublattice sites. While the vacancy is still predominantly constrained to the Li sublattice, its position around each Al between successive hops of the same Al is now more randomized, leading to an increase in the Al correlation factor above $x = 0.25$.

In conclusion, we have presented a first-principles method to calculate interdiffusion in binary alloys in which migration is mediated by vacancies. Applied to the fcc Al-Li alloy, our first-principles results have demonstrated the importance of the equilibruim degree of short- and long-range order in determining the kinetics of diffusion. The method presented in this Letter paves the way for the investigation of diffusional phase transformations with continuum simulations using thermodynamic and kinetic quantities calculated from first principles.

We are grateful for support from DOE, under Contract No. DE-FG02-96ER45571, and NSF supercomputing support (Grant No. ACI-9619020).

[1] D. de Fontaine, in *Solid State Physics*, (Academic, New York, 1994), p. 33; J. M. Sanchez, F. Ducastelle, and D. Gratias, Physica A (Amsterdam) **128**, 334 (1984).
[2] R. E. Howard and A. B. Lidiard, Rep. Prog. Phys. **27**, 161 (1964); A. R. Allnatt and A. B. Lidiard, Rep. Prog. Phys. **50**, 373 (1987).
[3] E. Nembach, Prog. Mater. Sci. **45**, 275 (2000).
[4] A. R. Allnatt, J. Phys. C **15**, 5605 (1982).
[5] J. W. Cahn and F. C. Larche, Scr. Metall. **17**, 927 (1983).
[6] K. W. Kehr, K. Binder, and S. M. Reulein, Phys. Rev. B **39**, 4891 (1989).
[7] M. H. F. Sluiter, Y. Watanabe, D. de Fontaine, and Y. Kawazoe, Phys. Rev. B **53**, 6137 (1996).
[8] G. Kresse and J. Furthmüller, Comput. Mater. Sci. **6**, 15 (1996).
[9] A. Van der Ven and G. Ceder, Phys. Rev. B (to be published).
[10] R. P. Elliott and F. A. Shunk, Bull. Alloy Phase Diagrams **2**, 353 (1981).
[11] This result is inconsistent with the traditional interpretation of the resistivity measurements of Ceresara *et al.*, Philos. Mag. **35**, 97 (1977).
[12] G. H. Vineyard, J. Phys. Chem. Solids **3**, 121 (1957).
[13] A. Van der Ven, G. Ceder, M. Asta, and P. D. Tepesch, Phys. Rev. B **64**, 184307 (2001).
[14] R. LeSar, R. Najafabadi, and D. J. Srolovitz, Phys. Rev. Lett. **63**, 624 (1989).
[15] See [13] and references therein for the algorithm. We used $8 \times 8 \times 8$ and $16 \times 16 \times 16$ cells containing one vacancy. L_{ij} is proportional to the vacancy concentration x_V for dilute x_V and the calculated L_{ij} were rescaled to a value corresponding to the equilibrium x_V. At each concentration, averages were performed over 400 different starting arrangements of Li and Al obtained with canonical Monte Carlo simulations.
[16] S. F. Baumann and D. B. Williams, Metall. Trans. A **16**, 1203, (1985).